Published in final edited form as:
J Neurochem. 2014 July ; 130(2): 185–198. doi:10.1111/jnc.12721.

α6β2*-subtype nicotinic acetylcholine receptors are more sensitive than α4β2*-subtype receptors to regulation by chronic nicotine administration

MJ Marks[1], **SR Grady**[1], **O Salminen**[2], **MA Paley**[1], **CR Wageman**[1], **JM McIntosh**[3], and **P Whiteaker**[4]

[1]Institute for Behavioral Genetics, 447 UCB, University of Colorado, Boulder, CO 80309
[2]Department of Pharmacy, Division of Pharmacology and Toxicology, University of Helsinki, Helsinki, Finland [3]George E. Wahlen Veterans Affairs Medical Center, Salt Lake City, Utah 84108, and Departments of Psychiatry and Biology, University of Utah, Salt Lake City, UT 84112
[4]Division of Neurobiology, Barrow Neurological Institute, St. Joseph's Hospital, Phoenix, AZ 85013

Abstract

Nicotinic acetylcholine receptors (nAChR) of the α6β2* subtype (where * indicates the possible presence of additional subunits) are prominently expressed on dopaminergic neurons. Because of this, their role in tobacco use and nicotine dependence has received much attention. Previous studies have demonstrated that α6β2*-nAChR are downregulated following chronic nicotine exposure (unlike other subtypes that have been investigated – most prominently α4β2* nAChR). This study examines, for the first time, effects across a comprehensive chronic nicotine dose range. Chronic nicotine dose-responses and quantitative ligand-binding autoradiography were used to define nicotine sensitivity of changes in α4β2*-nAChR and α6β2*-nAChR expression. α6β2*-nAChR downregulation by chronic nicotine exposure in dopaminergic and optic-tract nuclei was ≈three-fold more sensitive than upregulation of α4β2*-nAChR. In contrast, nAChR-mediated [^{3}H]-dopamine release from dopamine-terminal region synaptosomal preparations changed only in response to chronic treatment with high nicotine doses, while dopaminergic parameters (transporter expression and activity, dopamine receptor expression) were largely unchanged. Functional measures in olfactory tubercle preparations were made for the first time; both nAChR expression levels and nAChR-mediated functional measures changed differently between striatum and olfactory tubercles. These results show that functional changes measured using synaptosomal [^{3}H]-DA release are primarily due to changes in nAChR, rather than in dopaminergic, function.

Corresponding Author: Paul Whiteaker, Ph.D., Laboratory of Neurochemistry, Division of Neurobiology, Barrow Neurological Institute, St. Joseph's Hospital, Phoenix AZ 85013, USA, Tel: +1 602 406 6534, Fax: +1 602 406 4172, paul.whiteaker@dignityhealth.org.

The authors declare that they have no conflicts of interest associated with the work described in this manuscript.

Keywords

Dopaminergic terminal regions; nicotinic receptor; α4β2 subtype; dopamine transporter; dopamine receptor

Introduction

The effects of chronic nicotine exposure on nicotinic acetylcholine receptors (nAChR) have been the subject of many reports. It has been repeatedly demonstrated that chronic exposure to nicotine or tobacco smoke elicits an up-regulation of the number of α4β2-nAChR binding sites for many brain regions and in many species (Marks *et al.* 1983, Schwartz & Kellar 1983, Marks *et al.* 1992, Marks *et al.* 2011, Govind *et al.* 2009, Perry *et al.* 1999). However, some brain regions (such as thalamus and medial habenula) are less affected than others (such as cerebral cortex and hippocampus). The up-regulation occurs with no change in mRNA levels (Marks et al. 1992). The cellular processes underlying the up-regulation and the functional consequences of this up-regulation are complex and not fully understood. For example, the function of the α4β2*-nAChR has been shown to increase, decrease, or remain unchanged depending on the measure used (Jacobs *et al.* 2002, Grilli *et al.* 2005, Marks *et al.* 1993). Up-regulation of nAChR expression is not exhibited by every subtype. Specifically, down-regulation has been reported for the α6β2*-nAChR binding sites (Lai *et al.* 2005, Perry *et al.* 2007, Doura *et al.* 2008). Furthermore, the function of α6β2*-nAChR subtypes also appears to decrease or remain unchanged after chronic nicotine exposure (Lai et al. 2005, McCallum *et al.* 2006, Perry et al. 2007).

Differential nAChR subtype responses to chronic nicotine exposure are of particular importance in dopaminergic systems. Dopaminergic neurons express a variety of nicotinic receptor subtypes that contain α4β2*-nAChR-and/or α6β2*-nAChR-binding sites (Gotti *et al.* 2005, Champtiaux *et al.* 2003). Some of the α4β2*-nAChR also include the α5 subunit; the $(\alpha4\beta2)_2\alpha5$-nAChR subtype seems to be generally resistant to up-regulation (Mao *et al.* 2008, Moretti *et al.* 2010). In addition, $(\alpha4\beta2)_2\beta2$-nAChR sites located on dopaminergic neurons may not up-regulate (Nashmi *et al.* 2007). Consequently, up-regulation of α4β2*-nAChR sites in dopaminergic regions may be restricted to other types of neurons, perhaps GABAergic.

The α6β2*-nAChR are diverse and appear to respond differently to nicotine treatment. The subtype that contains both α4 and α6 subunits [(α4β2)(α6β2)β3] may down-regulate more than other α6β2-nAChR subtypes [$(\alpha6\beta2)_2\beta3$ and $(\alpha6\beta2)_2\beta2$] (Perez *et al.* 2008, Quik *et al.* 2011). Given the complexity and variety of nAChR subtypes expressed on dopaminergic neurons, it has been difficult to assess consequences of chronic nicotine exposure on this system. More recently, longer term chronic nicotine treatments by water bottle, minipump, and/or food, with or without cycles of withdrawal in mice, rats or monkeys have shown changes in reward behavior as well as changes in modulation of dopamine release by cyclic voltammetry methods (Zhang *et al.* 2012, Baker *et al.* 2013, Perez *et al.* 2012, Hilario *et al.* 2012, Bordia *et al.* 2013).

Several smoking cessation aids that target nicotinic acetylcholine receptors (nAChR) are in current use, including nicotine replacement by patch and gum, and varenicline, a partial agonist with high potency at the α4β2*-nAChR subtype. The sub-optimal efficacy of these treatments in achieving tobacco abstinence necessitates a search for other therapeutics, perhaps for alternative targets (Hurst *et al.* 2013, Pierce *et al.* 2012). Some of the less widely distributed nAChR subtypes have been proposed as targets. One of these is the α6β2*-nAChR with expression restricted mainly to dopaminergic and visual pathways (Brunzell 2012). This subtype regulates function of ventral tegmental area dopaminergic projection neurons, a pathway considered important in reward. Pharmacological manipulation of a more selective target, such as α6β2*-nAChR could be effective in aiding smoking cessation attempts with possibly fewer side effects. Availability of more detailed information about a target receptor should aid in designing better pharmacotherapies.

This study was undertaken to compare changes in both α4β2*-nAChR and α6β2*-nAChR binding sites as well as to evaluate functional changes resulting from variation of chronic nicotine treatment dose. We report that the chronic dose required for half-maximal change of α6β2*-nAChR site expression (decrease) was significantly lower than that required for half-maximal change of the α4β2*-nAChR sites (increase). In addition, binding site changes for both α6β2*-nAChR and α4β2*-nAChR-nAChR binding sites occur at lower chronic treatment doses than those leading to functional changes measured by nAChR-mediated [^{3}H]-dopamine release using synaptosomal preparations. In comparison to nAChR binding and functional parameters, measures of dopaminergic receptor expression and dopamine transporter were largely unchanged; we conclude that nAChR-level changes are likely primarily responsible for the observed effects of chronic nicotine on nAChR-mediated [^{3}H]-dopamine release.

Methods

Materials

[^{125}I]-Epibatidine (2200 Ci/mmol), [^{3}H]SCH23390 (N-methyl [^{3}H], 84.3 Ci/mmol), [^{3}H]mazindol (4'-[^{3}H], 20.6 Ci/mmol) and [^{3}H]raclopride (methoxy-[^{3}H], 20.6 Ci/mmol) were obtained from Perkin-Elmer NEN, Boston, MA. α-Conotoxin MII (α-CtxMII) and [^{125}I]-α-CtxMII were prepared as described previously (Whiteaker *et al.* 2000, Cartier *et al.* 1996). Unlabeled 5I-epibatidine was a generous gift from Dr. Kenneth Kellar, Georgetown University, Washington, DC. Liquid (−)-nicotine was purchased from Sigma-Aldrich Chemical Company (St. Louis, MO) and was redistilled periodically. All additional chemicals were of reagent grade.

Mice

Animal production methods and experimental procedures using mice were reviewed and approved by the Institutional Animal Care and Utilization Committee at the University of Colorado, Boulder. All mice were bred at the Institute for Behavioral Genetics, University of Colorado, Boulder. β2 null mutant mice (Picciotto *et al.* 1995) were originally obtained from Marina Picciotto, Yale University, New Haven, CT. Heterozygous mice were bred and pups genotyped from ear or tail clippings taken at weaning (21 days) (Salminen et al., 2004).

Mice were housed at 22°C with lights on from 7 AM to 7 PM and allowed free access to food and water.

Surgery

Cannulas were inserted in the right jugular vein of each mouse using previously published procedures (Barr *et al.* 1979). Briefly, mice were anesthesized with pentobarbital (50 mg/kg) and chloral hydrate (100 mg/kg). An incision exposed the superficial right jugular vein into which a silastic cannula (0.51 mm I.D. 0.94 mm O.D) was inserted. The cannula was passed through the back in the midscapular region and stabilized with surgical thread and a wound clip. The mouse was injected with buprenorphine (0.1 mg/kg), placed in a clean cage and warmed until wakening.

Nicotine Treatment

Mice were transferred to an individual infusion chambers and cannulas were connected to a 1 ml syringe mounted on an infusion pump (Harvard Apparatus, Holliston, MA). Sterile saline was continuously infused at a rate of 35μL/h for two days before nicotine treatment was begun. Mice were divided into seven treatment groups that received the following nicotine doses (free base as mg/kg/hr, prepared from liquid nicotine neutralized with HCl): 0 (saline-infused control), 0.125, 0.25, 0.5, 1.0, 2.0 or 4.0. This range of doses was chosen to maintain compatibility with our previous chronic nicotine treatment studies and to provide plasma nicotine concentrations that increase linearly with dose (Marks et al., 2004). In addition, since mice metabolize nicotine much faster than humans, plasma nicotine concentrations within the chosen dosing range will also cover the range of doses likely to be experienced by human smokers. The highest mouse dose (4.0 mg/kg/h) will produce an ≈ 1.2 μM plasma concentration; this slightly exceeds the upper end of the range seen in very heavy smokers (Matta *et al.* 2007, Marks *et al.* 2004). Following ten days of treatment with the indicated nicotine dose, nicotine treatment was discontinued and each cannula was checked for free fluid flow. A two hour interval of withdrawal was allowed before sacrifice to metabolize nicotine.(Petersen *et al.* 1984). Nicotine was used to gauge non-specific binding in the presence of 125I CtxMII (see also legend to Fig. 2).

Tissue Preparation

For samples to be prepared for sectioning, each mouse was killed by cervical dislocation, its brain was rapidly (<1 min) removed from the skull and quickly frozen by immersion in isopentane (−35°C) for 10 s. The frozen brain was wrapped in aluminum foil and stored at −70°C until sectioning.

Preparation of Tissue Sections

Frozen brains were removed from the −70°C freezer and allowed to warm to the temperature of the cryostat (−14°C) and mounted with M-1 Embedding Matrix (Anatomical Pathology, Pittsburgh, PA). Subsequently, 14 μm coronal sections were cut using either a Leica CM 1850 cryostat/microtome (Leica, Nussloch, Germany) or an IEC Minotome (Damon Corp., Needham, MA) and thaw mounted on Fisher Suprafrost/Plus microscope slides. A series of ten sets of slides were prepared from each brain to allow comparison of results for several

different experiments on adjacent or near-adjacent sections. Slides containing the brain sections were stored, desiccated at −70°C, until use.

[^{125}I]Epibatidine Autoradiography

Slides with tissue sections prepared were warmed to room temperature in a desiccators, transferred to Bel-Art (Wayne, NJ) slide racks that have been modified to hold 50 slides and rehydrated by incubation at 22°C for 15 min in isotonic buffer (NaCl, 144 mM; KCl, 2.2 mM, $CaCl_2$, 2.0 mM, $MgSO_4$, 1.0 mM; HEPES, 25 mM; pH = 7.5). Rehydrated slides were subsequently transferred to isotonic buffer containing 200 pM [^{125}I]epibatidine (specific activity 2200 Ci/mmol mixed with unlabeled 5I-epibatidine to yield a final specific activity of 220 Ci/mmol, a 10-fold dilution). Samples were incubated for 2 h at 22°C, then redistributed to slide racks containing 25 slides and washed as follows (all solutions at 4°C): Twice for 30 s in isotonic buffer, twice for 5 s in hypotonic buffer (0.1 ×) and twice for 5 s in 10 mM HEPES, pH = 7.5. Parallel series of sections were used to determine [^{125}I]epibatidine (200 pM) binding levels in the presence of 30 nM cytisine (sufficient to block binding to α4β2* nAChR, while leaving other subtypes unaffected (Whiteaker et al. 2000, Whiteaker *et al.* 2002)). Subsequently, slides were air dried and stored desiccated at room temperature in vacuum overnight before exposure initially to Packard Super Resolution Cyclone Storage Phosphor Screens to yield images for quantitation, and subsequently to Kodak MR autoradiography film (both from PerkinElmer, Inc., Waltham, MA) to yield higher resolution images for photography. Each Phosphor Screen was also simultaneously exposed to a series of tissue paste standards containing measured amounts of ^{125}I to allow quantitation of the image intensity. Tissue sections from β2 null mutant mice or samples incubated in the presence of 10 μM nicotine were used to establish blanks that did not differ from film background (Whiteaker *et al.* 2006).

[^{125}I]-α-CtxMII autoradiography

[^{125}I]-α-CtxMII binding was performed as previously described (Whiteaker et al. 2000). Sections were incubated for 10 min in binding buffer containing 1 mM phenylmethylsulfonyl fluoride (PMSF)). Sections were then incubated with 0.5 nM [^{125}I]-α-CtxMII in binding buffer with the addition of the protease inhibitors leupeptin, pepstatin, and aprotinin (10 μg/ml each) and bovine serum albumin (0.1% w/v), for 2 h at 22° C. Slides were subsequently washed in ice-cold protein free binding buffer twice for 30 s followed by two 10 s washes in 0.1× protein free binding buffer. Final rinses (2 × 5 s each) were conducted in ice-cold 5 mM HEPES, pH 7.5. Sections were subsequently air dried and desiccated overnight prior to exposure to Packard Phosphor screens and Kodak MR film as previously described for [^{125}I]epibatidine autoradiography. Tissue sections from β2 null mutant mice were again used to establish blanks.

Quantitation

Tissue paste samples prepared from whole brain homogenates containing measured amounts of ^{125}I were used to construct standard curves. The Phosphor screens produce a linear relationship between signal intensity and tissue radioactivity content over several orders of magnitude. The regression line calculated for the standard curve was used to convert the

measured value of pixels/mm^2 to the cpm/mg wet weight. Signal intensity in fmol/mg wet weight was estimated from the specific activity of each ligand. Brain regions were identified using a mouse brain atlas (Paxinos & Franklin 2004) as a guide. Multiple (4–6) measurements were made in each brain region of each mouse and the average of these measurements defined the signal intensity for each region.

Synaptosomal superfusion [^{3}H]-Dopamine release assay

Two dopamine terminal regions, striatum (ST) and olfactory tubercle (OT) were assessed for [^{3}H]-dopamine ([^{3}H]-DA) release from crude synaptosomes as previously described (Salminen *et al.* 2004, Salminen *et al.* 2007). These two regions were chosen as they are easily distinguished, rich sources of terminals from dopamine neurons originating in the substantia nigra (SN) and the ventral tegmental area (VTA), respectively. The OT and the nucleus accumbens both receive projections from similar areas of the VTA, and both regions respond similarly in drug-reward assessments (Ikemoto 2007). Nucleus accumbens was not used since sufficient material could only be obtained for functional assays by pooling samples from multiple mice. This was not practical given the demands of the chronic treatment experiments. Nicotine treatment was terminated at least two h before tissue preparation to allow metabolism of nicotine. For uptake of [^{3}H]-DA, crude synaptosomes were incubated at 37°C in uptake buffer (containing the following, in mM, 128 NaCl, 2.4 KCl, 3.2 $CaCl_2$, 1.2 KH_2PO_4, 1.2 $MgSO_4$, 25 HEPES, pH 7.5, 10 glucose, 1 ascorbic acid, and 0.01 pargyline) for 10 min before addition of 100 nM [^{3}H]-DA (1 μCi for every 0.2 ml of synaptosomes) and diisopropyl fluorophosphate (10 μM). The suspension was incubated for an additional 5 min. Aliquots of crude synaptosomes (80 μl) were distributed onto filters and superfused with buffer (uptake buffer containing 0.1% bovine serum albumin, 1 μM nomifensine and 1 μM atropine) at 0.7 ml/min for 10 min. For experiments using α-conotoxin MII (α-CtxMII) to inhibit α6β2*-nAChR, crude synaptosomes were exposed to α-CtxMII (50 nM) for the last 5 min of the 10 min buffer superfusion. This concentration of α-CtxMII inhibits all α6β2*-nAChR subtypes present in the mouse striatum (Salminen et al. 2007). [^{3}H]DA release mediated by α6β2*-nAChR was calculated as the difference between total release (in the absence of α-CtxMII) and α4β2*-nAChR-mediated release (retained in the presence of α-CtxMII). After buffer and/or α-CtxMII superfusion, crude synaptosomes were exposed to ACh for 20s. Basal and ACh-stimulated release was determined by collecting 23 × 10s fractions into 96-well plates.

Radioligand binding to membrane preparations

Expression levels of dopamine receptors and transporter were measured by binding of radioligands to membrane fractions isolated from olfactory tubercles or striata of mice treated with saline, 0.25, 1.0 or 4.0 mg/kg/h nicotine.

The expression of D1/D5 dopamine receptors was measured by membrane binding of [^{3}H]-SCH23390. Membrane preparations were incubated in binding buffer (30 μl volume including in mM: NaCl, 144; KCl, 1.5; CaCl2, 2; MgSO4, 1; HEPES, 20; pH=7.5). [^{3}H]-SCH23390 was used at 1.7 nM, (Kd ~ 0.1 nM), with 0.5 mM mianserin added to block binding to 5HT2 receptors, and 10 mM flupenthixol added for blank determination. Samples were incubated in 30 μL of binding buffer for 60 min at 22°C. Expression levels of D2/D3

dopamine receptors were measured with [^{3}H]-raclopride at 17 nM, (Kd ~ 2 nM) with 10 mM sulpiride added for blank determination. Assay volume and incubation time was identical to that used for determination of D1/D5 dopamine receptor expression, as was the bulk buffer composition.

Dopamine transporter (DAT) expression was measured by binding of [^{3}H]-mazindol (200 nM, Kd ~ 25 nM). Alternatively, for a small number of samples, [^{125}I]-RTI-121 (8 nM, Kd ~ 4 nM) was used. Fluoxetine (1 μM) and desipramine (100 nM) were used to block off-target binding to the serotonin and norepinephrine transporters, respectively. Blanks were determined using 100 mM nomifensine. Samples were incubated in 30 μL of binding buffer for 90 min at 22°C followed by 30 min at 4°C. Assay volumes were the same as for dopamine receptor assays, previously described.

Reactions were terminated by filtration of samples at 4°C onto a two layer filter consisting of one sheet of GFA/E glass fiber filter (Gelman Sciences, Ann Arbor, MI, U.S.A.) and one sheet of GF/B glass fiber filter (Micro Filtration Systems, Dublin, CA) both treated with 0.5% polyethylenimine using an Inotech Cell Harvester (Inotech, Rockville, MD, U.S.A.). Samples were subsequently washed six times with ice-cold binding buffer. Radioactivity was measured using a Wallac 1450 Microbeta scintillation counter (PerkinElmer Life and Analytical Sciences) after addition of 150 μl of Optiphase Supermix scintillation cocktail (PerkinElmer Life Sciences) to each well of a 96-well counting plate.

Dopamine transporter activity assays

Synaptosomes were prepared as for DA release assays. Synaptosomes were suspended in uptake buffer (in mM: NaCl, 128; KCl, 2.4; $CaCl_2$, 3.2; KH_2PO_4, 1.2; $MgSO_4$, 1.2; HEPES, 25, pH 7.5, glucose, 10; ascorbic acid, 1; and pargyline, 0.01) to a volume of 8 ml per mouse for ST and 4 ml per mouse for OT. Previously, we have determined the K_m concentration of DA for uptake into striatal synaptosomes of C57Bl6 mice to be 0.080 ± 0.003 mM (data not shown). Synaptosomes were incubated in uptake buffer (final volume 100 μl) with either 0.05 μM (close-to-K_d) or 1 μM (saturating concentration) of [^{3}H]-DA (40–55 Ci/mmol diluted with unlabeled DA to achieve concentration desired) at 22°C for 5 min. Nomifensine (100 μM) was used for blank determination. The reaction was terminated by filtration onto a two layer filter consisting of one sheet of GFA/E glass fiber filter (Gelman Sciences, Ann Arbor, MI, U.S.A.) and one sheet of GF/B glass fiber filter (Micro Filtration Systems, Dublin, CA) both soaked in uptake buffer. Samples were washed with cold uptake buffer four times. Radioactivity was measured using a Wallac 1450 Microbeta scintillation counter (PerkinElmer Life and Analytical Sciences) after addition of 150 μl of Optiphase Supermix scintillation cocktail (PerkinElmer Life Sciences) to each well of a 96-well counting plate.

Protein

Protein was measured using the method of Lowry et al (Lowry *et al.* 1951).

Statistical Analyses

SigmaPlot V9 (Systat Software, Inc., San Jose, CA) was used to derive assay parameters by nonlinear regression curve fitting. The following equations were used to examine the

decreases or increases in binding site density after chronic nicotine treatment: For decreases: $B_N = B_S/(1+nic/ED_{50}) + B_R$ and for increases: $B_N = B_S/(1+ED_{50}/nic) + B_{R:}$ where B_N is the binding measured following treatment with nicotine, B_S is the binding affected by the chronic nicotine treatment at the dosage = nic, ED_{50} is the nicotine treatment dose eliciting 50% of the maximal change and B_R is the binding unaffected by nicotine treatment.

The SPSS statistical package (IBM Corp., Somers, NY) was used for statistical analyses. Two-way ANOVAs (independent variables were nicotine treatment dose and brain region) were used to evaluate the effects of nicotine treatment on [^{125}I]epibatidine and [^{125}I]α-CtxMII binding. Subsequently, the effects of chronic nicotine treatment on binding site density were analyzed by nonlinear regression analysis as described above. One-way ANOVAs were also used to examine the effects of nicotine treatment on binding site density for each ligand in each brain region, and to evaluate the effects of chronic nicotine treatment on the binding of [^{3}H]SCH23390, [^{3}H]mazindol and [^{3}H]raclopride.

Results

The typical regional distribution of [^{125}I]α-CtxMII and [^{125}I]epibatidine binding is shown in Figure 1. Regions that were assessed by quantitative autoradiography are labeled. [^{125}I]α-CtxMII binding sites are prominently expressed in a limited set of brain nuclei, typically associated with optic tracts and dopamine projections originating in the substantia nigra and ventral tegmental area (Whiteaker et al. 2000). Within these regions, almost all [^{125}I]α-CtxMII binding sites correspond to α6β2* nAChR (Whiteaker *et al.* 2002, Gotti *et al.* 2005, Champtiaux *et al.* 2002).

[^{125}I]α-CtxMII binding sites are highly sensitive to downregulation by chronic nicotine exposure

[^{125}I]α-CtxMII binding site densities were determined in brains from mice exposed to a range of chronic nicotine doses (0 – 4 mg/kg/h for 10 d; see Methods for details). Regions with measurable [^{125}I]α-CtxMII binding were quantitated (see Figure 2). Chronic treatment with even low doses of nicotine produced downregulation of [^{125}I]α-CtxMII binding site expression in most regions (Figure 2). Comparison of binding levels by 2-way ANOVA indicated significant differences by Region, and by Dose, but no Dose × Region interaction (statistical analysis outcomes are provided in the legend to Table 1). Results were subsequently analyzed to evaluate the dose-dependence of the downregulation and calculate the extent of the downregulation. The mean ID_{50} value across regions exhibiting significant down regulation was 0.108 ± 0.040 mg/kg/h (see Table 1). This corresponds to a serum nicotine concentration of 35 nM (Marks *et al.* 2004). This analysis also provides an estimate of the maximal decrease in expression of [^{125}I]α-CtxMII binding sites and illustrates that chronic nicotine administration modestly, but significantly, reduces α6β2* nAChR expression across multiple regions (mean of 5 regions analyzed −24.1 ± 1.2% of saline control, see Table 1). Optic tracts and superior colliculus (for which regions no significant effect of nicotine treatment was observed) were not included.

Cytisine-sensitive [^{125}I]Epibatidine binding sites are less sensitive to upregulation by chronic nicotine exposure

Expression of cytisine-sensitive [^{125}I]epibatidine binding sites (corresponding to α4β2* nAChR) was generally upregulated by chronic nicotine treatment (Figure 3) in the same regions that showed downregulation of [^{125}I]α-CtxMII binding sites (corresponding to α6β2* nAChR). Note that [^{125}I]epibatidine binding data are shown for 7 of the 8 regions analyzed for [^{125}I]α-CtxMII binding plus 2 cortical regions. Optic tract [^{125}I]epibatidine binding could not be distinguished from [^{125}I]epibatidine binding to the adjacent thalamic region. Comparison by 2-way ANOVA of the effects of chronic nicotine treatment on [^{125}I]epibatidine binding levels in the brain regions listed in Table 1 indicated significant differences by Region, and by Dose, but no Dose × Region interaction (statistical analysis outcomes are provided in the legend to Table 1). As for [^{125}I]α-CtxMII binding sites, levels of α4β2* nAChR expression vary between regions of interest, and are affected by chronic nicotine administration (although expression changes are opposite in direction between the two nAChR populations). Analysis of the dose dependence for upregulation of [^{125}I]epibatidine binding by nonlinear regression indicated that higher doses of nicotine were required to upregulate α4β2* nAChR expression than to downregulate α6β2*-nAChR expression. The mean ED_{50} value across 7 regions with significant response to nicotine treatment was 0.293 ± 0.027 mg/kg/h (see Table 1). This corresponds to a serum nicotine concentration of 95 nM (Marks *et al.* 2004), which is ~3-fold higher than the ID_{50} value for the [^{125}I]α-CtxMII binding downregulation. The extent of upregulation varied from a 47% to a 93% increase for regions with significant changes (mean for 7 regions, +72.5 ± 5.9%, see Table 1).

Chronic exposure to nicotine doses reduces α6β2* nAChR-mediated [^{3}H]DA release from striatal synaptosomes

The effects of chronic nicotine treatment on α-CtxMII-sensitive (α6β2*) nAChR function were assessed using [^{3}H]DA release from striatal and olfactory tubercle synaptosomal preparations. Chronic nicotine treatment doses were chosen that corresponded to partial α6β2* downregulation (0.25 mg/kg/h), partial α4β2 upregulation (1 mg/kg/h), or full effect on both (4 mg/kg/h). The outcomes of these experiments are illustrated in Figure 4.

In the striatum, only the very highest dose of chronic nicotine treatment produced a significant change in the amount of nicotine-evoked α6β2*-nAChR-mediated [^{3}H]-DA release (see Table 2) [^{3}H]-DA release EC_{50} values, while trending downward, were not significantly changed with any of the treatments. In contrast, no statistical differences were detected by one-way ANOVA in nicotine-evoked α6β2*-nAChR-mediated release parameters from olfactory tubercle preparations at any chronic nicotine dose. Statistical analysis is presented in the legend to Table 2.

Chronic exposure to nicotine reduces α4β2* nAChR-mediated [^{3}H]DA release from striatal and olfactory tubercle synaptosomes

The effects of chronic nicotine treatment on α-CtxMII-resistant (α4β2*) nAChR function were also determined, using [^{3}H]DA release from striatal and olfactory tubercle synaptosomal preparations. The same chronic nicotine doses were used as for assessment of

α6β2* nAChR function. The results are shown in Figure 5. Note that the relative errors associated with the measurements are small for α-CtxMII-resistant (α4β2* nAChR) function compared to determinations of α-CtxMII-sensitive (α6β2* nAChR) function since the latter is calculated as the difference between two measures (total and α-CtxMII-resistant function).

For striatal synaptosomes, the two highest chronic nicotine treatment doses elicited significant decreases in the amount of nicotine-evoked α4β2*-nAChR-mediated [^{3}H]-DA release (see Table 2). This contrasts with the effects on striatal α6β2* nAChR mediated function, for which function as well as amount of binding was reduced; whereas reductions in α4β2*-nAChR-mediated [^{3}H]-DA release are seen even though binding sites are increased. Furthermore, only the highest dose of nicotine significantly changed either function, even though half-maximal values for changing binding are considerably lower. No significant effect of chronic nicotine treatment was seen on α6β2*- or α4β2*-nAChR-mediated [^{3}H]-DA release EC_{50} values (see Table 2). Similar significant decreases were seen for α4β2*-mediated function in olfactory tubercle synaptosomal preparations following treatment with the highest nicotine dose.

Chronic nicotine treatment does not affect dopamine receptor or transporter expression in striatum or olfactory tubercles

As previously described, chronic nicotine treatment elicited changes in nAChR-mediated dopamine release from striatal and olfactory tubercle synaptosomal preparations. This effect might reflect changes in either nAChR function or be due to changes in dopaminergic parameters induced by chronic nicotine treatment. Accordingly, we assessed expression of D1/D5 dopamine receptors (using [^{3}H]SCH-23390), of D2/D4 dopamine receptors (using [^{3}H]raclopride), and of DAT (using [^{3}H]mazindol) in membrane preparations from these two regions. As shown in Figure 6, none of these dopaminergic markers were changed by chronic nicotine treatment across the dose range that altered nAChR-mediated synaptosomal [^{3}H]dopamine release.

Dopamine transporter function in striatum and olfactory tubercles is generally resistant to the effects of chronic nicotine treatment

In a further examination of possible chronic nicotine treatment effects on dopaminergic parameters, DAT activity was also measured in striatal and olfactory tubercle synaptosomal preparations. As shown in Table 3, almost all measures of dopamine transporter activity were unaffected by chronic nicotine treatment. The rate of [^{3}H]-DA uptake was measured following 5 min incubations using of [^{3}H]-DA concentrations at approximately K_m (50 nM), or at a saturating concentration (1 μM). Rates of uptake were not altered at any chronic nicotine dose. Equilibrium [^{3}H]-DA uptake was also measured at 30 min, using the same substrate concentrations. In striatum, total uptake was unaltered by chronic nicotine for either [^{3}H]-DA concentration. A similar outcome was observed for total uptake of 50 nM [^{3}H]-DA in olfactory tubercle. However, at the highest (4 mg/kg/h) chronic nicotine dose only, olfactory tubercle synaptosomal [^{3}H]-DA uptake was significantly increased compared to the saline-treated control preparation. The use of two different [^{3}H]-DA concentrations allows an estimate to be made of whether the DAT K_m for dopamine uptake has changed. A

ratio of ~K_m concentration / saturating concentration uptake should remain at approximately 2. As shown in Table 3, this is indeed the case; no significant changes in uptake ratio were observed for region or treatment for either rate or total amount of [^{3}H]-DA uptake. We conclude that the DAT affinity for [^{3}H]-DA uptake is not altered by chronic nicotine treatment in either region, under any of the conditions tested.

Discussion

This study represents the first comprehensive examination of dose-response relationships performed for downregulation of murine [^{125}I]α-CtxMII binding sites (corresponding to α6β2*- nAChR) by chronic nicotine treatment. Importantly, the ID_{50} values for downregulation and the extent of downregulation are very similar in the multiple nuclei in those dopaminergic and optic tracts responding to chronic nicotine treatment. Although previous studies have not examined the effect of nicotine dose on α6β2*-nAChR, where points of comparison are available, the current data (summarized in Table 1) generally agree well with those from previous studies. In striatum, downregulation of α6β2* nAChR expression by chronic nicotine treatment has reliably been observed across multiple animal models. For example, in rat striatum declines of −3% (Nguyen et al. 2003), −33% (Mugnaini *et al.* 2006), −28% (Perry *et al.* 2007) and −27% (Doura et al, 2008) vs. control were seen in α6β2*-nAChR expression frequently using nicotine administration (6 mg/kg/day) with osmotic minipumps. Owing to differences in metabolism, this treatment is estimated provide plasma nicotine concentrations comparable to those following treatment of mice with a dose of 2.5 mg/kg/hr (Matta et al., 2007). The plasma nicotine level measured in one study was 1.91 μM (Doura et al., 2008) almost twice that attained in the plasma of mice treated with the highest nicotine dose (1.2 μM after 4 mg/kg/hr) used in the current study (Marks et al., 2004). Thus the apparently high doses that we used to treat the mice yield steady-state nicotine concentrations comparable to those achieved with the much lower doses used in rats. Declines have also been reported for striatal binding in mice chronically treated with nicotine: −30%, −28%, and −30% (Quik *et al.* 2012). Finally in squirrel monkey striatum, chronic nicotine treatment resulted in a −20% decline compared to control (McCallum *et al.* 2006). As another point of comparison, we observed little change in superior colliculus α6β2* nAChR expression following chronic nicotine administration. This is supported by three previous rat studies which also report modest declines: −2% (Perry et al. 2007), −10% (Mugnaini et al. 2006) and −2.9% (Doura et al., 2008). In the current study, we show that relatively low doses elicit declines in α6β2*-nAChR expression (declines plateau after approx 0.5 mg/kg/hr). The studies previously cited generally used doses comparable to our higher treatment doses, so decreases in expression can be compared to the maximum decreases observed in the current work.

Consistent with numerous previous reports, chronic nicotine treatment upregulated α4β2* nAChR expression. This phenomenon was first observed thirty years ago (Schwartz & Kellar 1983, Marks *et al.* 1983), and provides a valuable demonstration that the chronic nicotine treatment protocol worked as intended. The observed ED_{50} values for α4β2*-nAChR upregulation (Table 1) also match well with our recent publication (Marks *et al.* 2011), which demonstrated that this phenomenon is caused by increased expression of

nAChR protein. The ED_{50} value for α4β2* nAChR upregulation by chronic nicotine treatment (95 nM) was ≈3× higher than the ID_{50} value for α6β2* downregulation (35 nM).

The downregulation or α6β2* nAChR sites is thus exceptionally sensitive. For comparison, plasma nicotine concentrations in smokers are typically 150 – 250 nM post smoking, and fall as low as 6 nM following overnight abstinence (Jarvik *et al.* 2000). On this basis, α4β2*-nAChR will be exposed to a ≈ED_{50} (for upregulation) nicotine concentration for significant parts of the day, but well below overnight (although CNS levels will be somewhat higher than plasma levels). α6β2*-nAChR, however, will be at a >ID_{50} downregulation concentration for the whole day and much of the night.

Both α6β2*- and α4β2*-nAChR are expressed on striatal and olfactory tubercle dopamine terminals. This allowed the use of the long-established synaptosomal [^{3}H]-DA release technique to assess the impact of chronic nicotine treatment on α6β2*- and α4β2*-nAChR function. Mice were withdrawn from nicotine treatment for 2 hr before tissue preparation, which should allow sufficient time between cessation of treatment and functional assessment for nicotine to be metabolized. Functional effects are thus a consequence of chronic treatment, not of residual nicotine. Intriguingly, dopamine-terminal α6β2*-nAChR function appeared to be more sensitive to reduction by chronic nicotine in striatum where dopamine terminals are projections from the SN than in the olfactory tubercles where terminals are from the VTA. Even in striatal samples, only the highest dose (4 mg/kg/h) affected the total nAChR-mediated [^{3}H]-DA release. The decrease in function resembled that seen for high (single) doses tested in previous studies: −35% (Lai et al. 2005) and ≈50% (Quik et al. 2012) in mice, and −54% in rats (Perry et al. 2007). However, the chronic nicotine dose required to downregulate α6β2*-nAChR function was much greater than that required to downregulate expression. It therefore seems unlikely that loss of receptors *per se* is solely responsible for loss of function. This disconnect raised the question of whether changes in α6β2* nAChR composition might underlie the observed loss of function (perhaps due to changes in incorporation of α4 and/or β3 subunits that commonly co-assemble into α6β2*-nAChR (Gotti et al. 2005)). Since α6β2* nAChR are a mixed population of related subtypes, it is possible that individual subtypes may be differentially regulated by chronic nicotine treatment. It has been shown that α6β2β3* nAChR are more sensitive to downregulation at high (560 nM) serum nicotine concentrations than are α6β2*(no β3)-nAChR (Perry et al. 2007). In addition, α6α4β2*-nAChR appear to be more sensitive to chronic nicotine downregulation than are α6β2*(no α4)-nAChR (Perez et al. 2008). In contrast, our results indicated no significant changes EC_{50} values of nicotine evoked [^{3}H]-DA release for either striatal or olfactory tubercle synaptosomes, at any chronic nicotine dose (as might be expected if subtype composition was changed following chronic treatment (Salminen et al. 2007)). However, a small change in the ratio of populations with rather similar EC_{50} values (Salminen et al. 2007) may not be detectable. In addition, the total amount of nicotine evoked [^{3}H]-DA release was unchanged for olfactory tubercle, but decreased for striatum. No previous studies exist to provide points of comparison, but the regional difference is striking. Perhaps the olfactory tubercle α6β2*-nAChR population more-closely resembles that in the treated striatum. However, striatal EC_{50} values tended to fall with chronic nicotine treatment, moving further away from those measured in OT, rather than converging.

Alternatively, α6β2*-nAChR in the two regions may be subject to different regulation mechanisms, in which case the observed differences may be context- rather than receptor-dependent.

The overall magnitude of effects on maximal α4β2*-nAChR function in striatum is less than for α6β2*-nAChR. This also corresponds well to results for mouse striatum from previous studies: no change (Lai et al. 2005) or a ≈30% decrease in [^{3}H]-DA release at high stimulating agonist concentrations only (Quik et al. 2012). No functional change was seen in rat striatum (Perry et al. 2007). Again, no previous studies are available for comparison to our results in olfactory tubercle.

The changes in α6β2*- and α4β2*-nAChR-mediated [^{3}H]-DA release following chronic nicotine treatment could be due to alterations in nAChR function, or to changes in dopaminergic system parameters. However, no changes in dopamine receptor or transporter expression levels were seen at any chronic nicotine treatment dose. Further, no evidence was seen for changes in DAT affinity for dopamine, and only in one set of conditions (total equilibrium uptake of [^{3}H]-DA in olfactory tubercles following chronic treatment at the highest nicotine dose) was transporter activity significantly changed. We note that despite this change in DAT-mediated uptake, α6β2* nAChR-mediated [^{3}H]-DA release from olfactory tubercle synaptosomes remained unchanged under the same chronic treatment regime, while [^{3}H]-DA release mediated by α4β2* nAChR decreased similarly to striatum (Table 2). Although equivalent experiments have not been performed previously in olfactory tubercle, previous studies in striatum are in general agreement with our current observations. No changes in striatal DAT binding or overall dopamine levels were found following chronic nicotine treatment in squirrel monkeys (Perez *et al.* 2009), or for DAT binding or dopamine uptake as measured by voltammetry (Perez *et al.* 2012). A similar lack of effect on DAT binding levels was also observed in mice (Quik et al. 2012).

Taken together, our findings indicate that functional changes (as measured using synaptosomal [^{3}H]-DA release) are due more directly to changes in nAChR function, than in dopaminergic function *per se*. Our work expands on previous studies by examining effects across a comprehensive chronic nicotine treatment dose range, and by measuring α6β2*- and α4β2*-nAChR function in olfactory tubercle as well as striatal preparations. Intriguingly, nAChR populations in these two regions respond differently (both in terms of changing expression levels and of function) to chronic nicotine treatment. This finding resembles earlier observations of disparate responses in different regions of non-human primate caudate-putamen. The observed significant differences in ED/ID$_{50}$ values and direction for changes in α4β2* and α6β2* nAChR expression may result in notable changes in system/circuit equilibrium, since α4β2 nAChR are also expressed on GABA terminals that affect function in dopamine projection areas (English *et al.* 2012, Luo *et al.* 2013), while α6β2* nAChR are found only on the dopamine projections themselves (Gotti et al. 2005, Quik *et al.* 2005, Gotti *et al.* 2010).

Acknowledgments

This study was primarily supported by NIH grant R01 DA012242 (to PW). Additional support was provided by NIH grants R01 GM103801 and P01 GM48677 (to JMM).

Abbreviations

α-Ctx	α-conotoxin
A85380	3-((2S)-azetidinylmethoxy)pyridine
DA	dopamine
DAT	dopamine transporter
DLG	dorsolateral geniculate nucleus
HEPES	2-[4-(2-hydroxyethyl)piperazin-1-yl]ethanesulfonic acid
mHab	medial habunula
nAcc, nAChR	nicotinic acetylcholine receptor; nucleus accumbens
opt	optic tract
OPTN	olivary pretectal nucleus
OT	olfactory tubercle
PMSF	phenylmethylsulfonyl fluoride
SC	superior colliculus (superficial layers)
SCH23390	7-chloro-3-methyl-1-phenyl-1,2,4,5-tetrahydro-3-benzazepin-8-ol
Str	striatum
Th	thalamus
VLGN	ventrolateral geniculate nucleus
VTA	ventral tegmental area

Literature Cited

Baker LK, Mao D, Chi H, et al. Intermittent nicotine exposure upregulates nAChRs in VTA dopamine neurons and sensitises locomotor responding to the drug. European Journal of Neuroscience. 2013; 37:1004–1011. [PubMed: 23331514]

Barr JE, Holmes DB, Ryan LJ, Sharpless SK. Techniques for the chronic cannulation of the jugular vein in mice. Pharmacol Biochem Behav. 1979; 11:115–118. [PubMed: 493295]

Bordia T, McIntosh JM, Quik M. The nicotine-mediated decline in l-dopa-induced dyskinesias is associated with a decrease in striatal dopamine release. J Neurochem. 2013; 125:291–302.

Brunzell DH. Preclinical Evidence That Activation of Mesolimbic Alpha 6 Subunit Containing Nicotinic Acetylcholine Receptors Supports Nicotine Addiction Phenotype. Nicotine & Tobacco Research. 2012; 14:1258–1269. [PubMed: 22492084]

Cartier GE, Yoshikami D, Gray WR, Luo S, Olivera BM, McIntosh JM. A new alpha-conotoxin which targets alpha3beta2 nicotinic acetylcholine receptors. J Biol Chem. 1996; 271:7522–7528. [PubMed: 8631783]

Champtiaux N, Gotti C, Cordero-Erausquin M, et al. Subunit composition of functional nicotinic receptors in dopaminergic neurons investigated with knock-out mice. Journal of Neuroscience. 2003; 23:7820–7829. [PubMed: 12944511]

Champtiaux N, Han ZY, Bessis A, Rossi FM, Zoli M, Marubio L, McIntosh JM, Changeux JP. Distribution and pharmacology of alpha 6-containing nicotinic acetylcholine receptors analyzed with mutant mice. Journal of Neuroscience. 2002; 22:1208–1217. [PubMed: 11850448]

Doura MB, Gold AB, Keller AB, Perry DC. Adult and periadolescent rats differ in expression of nicotinic cholinergic receptor subtypes and in the response of these subtypes to chronic nicotine exposure. Brain research. 2008; 1215:40–52. [PubMed: 18474362]

English DF, Ibanez-Sandoval O, Stark E, Tecuapetla F, Buzsaki G, Deisseroth K, Tepper JM, Koos T. GABAergic circuits mediate the reinforcement-related signals of striatal cholinergic interneurons. Nat Neurosci. 2012; 15:123–U155. [PubMed: 22158514]

Gotti C, Guiducci S, Tedesco V, et al. Nicotinic Acetylcholine Receptors in the Mesolimbic Pathway: Primary Role of Ventral Tegmental Area alpha 6 beta 2*Receptors in Mediating Systemic Nicotine Effects on Dopamine Release, Locomotion, and Reinforcement. Journal of Neuroscience. 2010; 30:5311–5325. [PubMed: 20392953]

Gotti C, Moretti M, Clementi F, Riganti L, McIntosh JM, Collins AC, Marks MJ, Whiteaker P. Expression of nigrostriatal alpha 6-containing nicotinic acetylcholine receptors is selectively reduced, but not eliminated, by beta 3 subunit gene deletion. Molecular pharmacology. 2005; 67:2007–2015. [PubMed: 15749993]

Govind AP, Vezina P, Green WN. Nicotine-induced upregulation of nicotinic receptors: Underlying mechanisms and relevance to nicotine addiction. Biochemical pharmacology. 2009; 78:756–765. [PubMed: 19540212]

Grilli M, Parodi M, Raiteri M, Marchi M. Chronic nicotine differentially affects the function of nicotinic receptor subtypes regulating neurotransmitter release. J Neurochem. 2005; 93:1353–1360. [PubMed: 15934954]

Hilario MRF, Turner JR, Blendy JA. Reward Sensitization: Effects of Repeated Nicotine Exposure and Withdrawal in Mice. Neuropsychopharmacology. 2012; 37:2661–2670. [PubMed: 22828747]

Hurst R, Rollema H, Bertrand D. Nicotinic acetylcholine receptors: From basic science to therapeutics. Pharmacology & Therapeutics. 2013; 137:22–54. [PubMed: 22925690]

Ikemoto S. Dopamine reward circuitry: Two projection systems from the ventral midbrain to the nucleus accumbens–olfactory tubercle complex. Brain Research Reviews. 2007; 56:27–78. [PubMed: 17574681]

Jacobs I, Anderson DJ, Surowy CS, Puttfarcken PS. Differential regulation of nicotinic receptor-mediated neurotransmitter release following chronic (−)-nicotine administration. Neuropharmacology. 2002; 43:847–856. [PubMed: 12384170]

Jarvik ME, Madsen DC, Olmstead RE, Iwamoto-Schaap PN, Elins JL, Benowitz NL. Nicotine blood levels and subjective craving for cigarettes. Pharmacol. Biochem. Behav. 2000; 66:553–558. [PubMed: 10899369]

Lai A, Parameswaran N, Khwaja M, Whiteaker P, Lindstrom JM, Fan H, McIntosh JM, Grady SR, Quik M. Long-term nicotine treatment decreases striatal alpha 6 nicotinic acetylcholine receptor sites and function in mice. Molecular pharmacology. 2005; 67:1639–1647. [PubMed: 15681595]

Lowry OH, Rosebrough NJ, Farr AL, Randall RJ. Protein measurement with the Folin phenol reagent. J Biol Chem. 1951; 193:265–275. [PubMed: 14907713]

Luo RX, Janssen MJ, Partridge JG, Vicini S. Direct and GABA-mediated indirect effects of nicotinic ACh receptor agonists on striatal neurones. Journal of Physiology-London. 2013; 591:203–217.

Mao D, Perry DC, Yasuda RP, Wolfe BB, Kellar KJ. The α4β2α5 nicotinic cholinergic receptor in rat brain is resistant to up-regulation by nicotine in vivo. J Neurochem. 2008; 104:446–456. [PubMed: 17961152]

Marks MJ, Burch JB, Collins AC. Effects of chronic nicotine infusion on tolerance development and nicotinic receptors. Journal of Pharmacology and Experimental Therapeutics. 1983; 226:817–825. [PubMed: 6887012]

Marks MJ, Grady SR, Collins AC. Downregulation of nicotinic receptor function after chronic nicotine infusion. Journal of Pharmacology and Experimental Therapeutics. 1993; 266:1268–1276. [PubMed: 8371136]

Marks MJ, McClure-Begley TD, Whiteaker P, Salminen O, Brown RWB, Cooper J, Collins AC, Lindstrom JM. Increased Nicotinic Acetylcholine Receptor Protein Underlies Chronic Nicotine-Induced Up-Regulation of Nicotinic Agonist Binding Sites in Mouse Brain. Journal of Pharmacology and Experimental Therapeutics. 2011; 337:187–200. [PubMed: 21228066]

Marks MJ, Pauly JR, Gross SD, Deneris ES, Hermansborgmeyer I, Heinemann SF, Collins AC. Nicotine Binding and Nicotinic Receptor Subunit Rna after Chronic Nicotine Treatment. Journal of Neuroscience. 1992; 12:2765–2784. [PubMed: 1613557]

Marks MJ, Rowell PP, Cao JZ, Grady SR, McCallum SE, Collins AC. Subsets of acetylcholine-stimulated 86Rb(+) efflux and [I-125]-epibatidine binding sites in C57BL/6 mouse brain are differentially affected by chronic nicotine treatment. Neuropharmacology. 2004; 46:1141–1157. [PubMed: 15111021]

Matta SG, Balfour DJ, Benowitz NL, et al. Guidelines on nicotine dose selection for in vivo research. Psychopharmacology. 2007; 190:269–319. [PubMed: 16896961]

McCallum SE, Parameswaran N, Bordia T, Fan H, McIntosh JM, Quik M. Differential Regulation of Mesolimbic α3/α6β2 and α4β2 Nicotinic Acetylcholine Receptor Sites and Function after Long-Term Oral Nicotine to Monkeys. Journal of Pharmacology and Experimental Therapeutics. 2006; 318:381–388. [PubMed: 16622038]

Moretti M, Mugnaini M, Tessari M, Zoli M, Gaimarri A, Manfredi I, Pistillo F, Clementi F, Gotti C. A Comparative Study of the Effects of the Intravenous Self- Administration or Subcutaneous Minipump Infusion of Nicotine on the Expression of Brain Neuronal Nicotinic Receptor Subtypes. Molecular pharmacology. 2010; 78:287–296. [PubMed: 20439469]

Mugnaini M, Garzotti M, Sartori I, Pilla M, Repeto P, Heidbreder CA, Tessari M. Selective down-regulation of [125I]Y0-α-conotoxin MII binding in rat mesostriatal dopamine pathway following continuous infusion of nicotine. Neuroscience. 2006; 137:565–572. [PubMed: 16289885]

Nashmi R, Xiao C, Deshpande P, et al. Chronic nicotine cell specifically upregulates functional alpha 4*nicotinic receptors: Basis for both tolerance in midbrain and enhanced long-term potentiation in perforant path. Journal of Neuroscience. 2007; 27:8202–8218. [PubMed: 17670967]

Nguyen HN, Rasmussen BA, Perry DC. Subtype-Selective Up-Regulation by Chronic Nicotine of High-Affinity Nicotinic Receptors in Rat Brain Demonstrated by Receptor Autoradiography. Journal of Pharmacology and Experimental Therapeutics. 2003; 307:1090–1097. [PubMed: 14560040]

Paxinos, G.; Franklin, KBJ. The Mouse Brain in Stereotaxic Coordinates. Elsevier Academic Press; 2004.

Perez XA, Bordia T, McIntosh JM, Grady SR, Quik M. Long-Term Nicotine Treatment Differentially Regulates Striatal α6α4β2* and α6(Nonα4)β2* nAChR Expression and Function. Molecular pharmacology. 2008; 74:844–853. [PubMed: 18583454]

Perez XA, Ly J, McIntosh JM, Quik M. Long-Term Nicotine Exposure Depresses Dopamine Release in Nonhuman Primate Nucleus Accumbens. Journal of Pharmacology and Experimental Therapeutics. 2012; 342:335–344. [PubMed: 22562772]

Perez XA, O'Leary KT, Parameswaran N, McIntosh JM, Quik M. Prominent Role of alpha 3/alpha 6 beta 2*nAChRs in Regulating Evoked Dopamine Release in Primate Putamen: Effect of Long-Term Nicotine Treatment. Molecular pharmacology. 2009; 75:938–946. [PubMed: 19144785]

Perry DC, Dávila-GarcÍa MI, Stockmeier CA, Kellar KJ. Increased Nicotinic Receptors in Brains from Smokers: Membrane Binding and Autoradiography Studies. Journal of Pharmacology and Experimental Therapeutics. 1999; 289:1545–1552. [PubMed: 10336551]

Perry DC, Mao DY, Gold AB, McIntosh JM, Pezzullo JC, Kellar KJ. Chronic nicotine differentially regulates alpha 6-and beta 3-containing nicotinic cholinergic receptors in rat brain. Journal of Pharmacology and Experimental Therapeutics. 2007; 322:306–315. [PubMed: 17446303]

Petersen DR, Norris KJ, Thompson JA. A comparative study of the disposition of nicotine and its metabolites in three inbred strains of mice. Drug Metab Dispos. 1984; 12:725–731. [PubMed: 6150822]

Picciotto MR, Zoli M, Lena C, et al. Abnormal avoidance learning in mice lacking functional high-affinity nicotine receptor in the brain. Nature. 1995; 374:65–67. [PubMed: 7870173]

Pierce CR, O'Brien CP, Kenny PJ, Vanderschuren LJMJ. Rational Development of Addiction Pharmacotherapies: Successes, Failures, and Prospects. Cold Spring Harbor Perspectives in Medicine. 2012; 2

Quik M, Park KM, Hrachova M, Mallela A, Huang LZ, McIntosh JM, Grady SR. Role for α6 nicotinic receptors in l-dopa-induced dyskinesias in parkinsonian mice. Neuropharmacology. 2012; 63:450–459. [PubMed: 22579614]

Quik M, Perez XA, Grady SR. Role of alpha 6 nicotinic receptors in CNS dopaminergic function: relevance to addiction and neurological disorders. Biochemical pharmacology. 2011; 82:873–882. [PubMed: 21684266]

Quik M, Vailati S, Bordia T, Kulak JM, Fan H, McIntosh JM, Clementi F, Gotti C. Subunit composition of nicotinic receptors in monkey striatum: Effect of treatments with 1-Methyl-4-phenyl-1,2,3,6-tetrahydropyridine or L-DOPA. Molecular pharmacology. 2005; 67:32–41. [PubMed: 15470079]

Salminen O, Drapeau JA, McIntosh JM, Collins AC, Marks MJ, Grady SR. Pharmacology of alpha-conotoxin MII-sensitive subtypes of nicotinic acetylcholine receptors isolated by breeding of null mutant mice. Mol Pharmacol. 2007; 71:1563–1571. [PubMed: 17341654]

Salminen O, Murphy KL, McIntosh JM, Drago J, Marks MJ, Collins AC, Grady SR. Subunit composition and pharmacology of two classes of striatal presynaptic nicotinic acetylcholine receptors mediating dopamine release in mice. Mol Pharmacol. 2004; 65:1526–1535. [PubMed: 15155845]

Schwartz RD, Kellar KJ. Nicotinic cholinergic receptor-binding sites in the brain - regulation *in vivo*. Science. 1983; 220:214–216. [PubMed: 6828889]

Whiteaker P, Cooper JF, Salminen O, Marks MJ, McClure-Begley TD, Brown RW, Collins AC, Lindstrom JM. Immunolabeling demonstrates the interdependence of mouse brain alpha4 and beta2 nicotinic acetylcholine receptor subunit expression. J Comp Neurol. 2006; 499:1016–1038. [PubMed: 17072836]

Whiteaker P, McIntosh JM, Luo S, Collins AC, Marks MJ. 125I-alpha-conotoxin MII identifies a novel nicotinic acetylcholine receptor population in mouse brain. Mol Pharmacol. 2000; 57:913–925. [PubMed: 10779374]

Whiteaker P, Peterson CG, Xu W, McIntosh JM, Paylor R, Beaudet AL, Collins AC, Marks MJ. Involvement of the alpha 3 subunit in central nicotinic binding populations. Journal of Neuroscience. 2002; 22:2522–2529. [PubMed: 11923417]

Zhang L, Dong Y, Doyon WM, Dani JA. Withdrawal from Chronic Nicotine Exposure Alters Dopamine Signaling Dynamics in the Nucleus Accumbens. Biological Psychiatry. 2012; 71:184–191. [PubMed: 21872847]

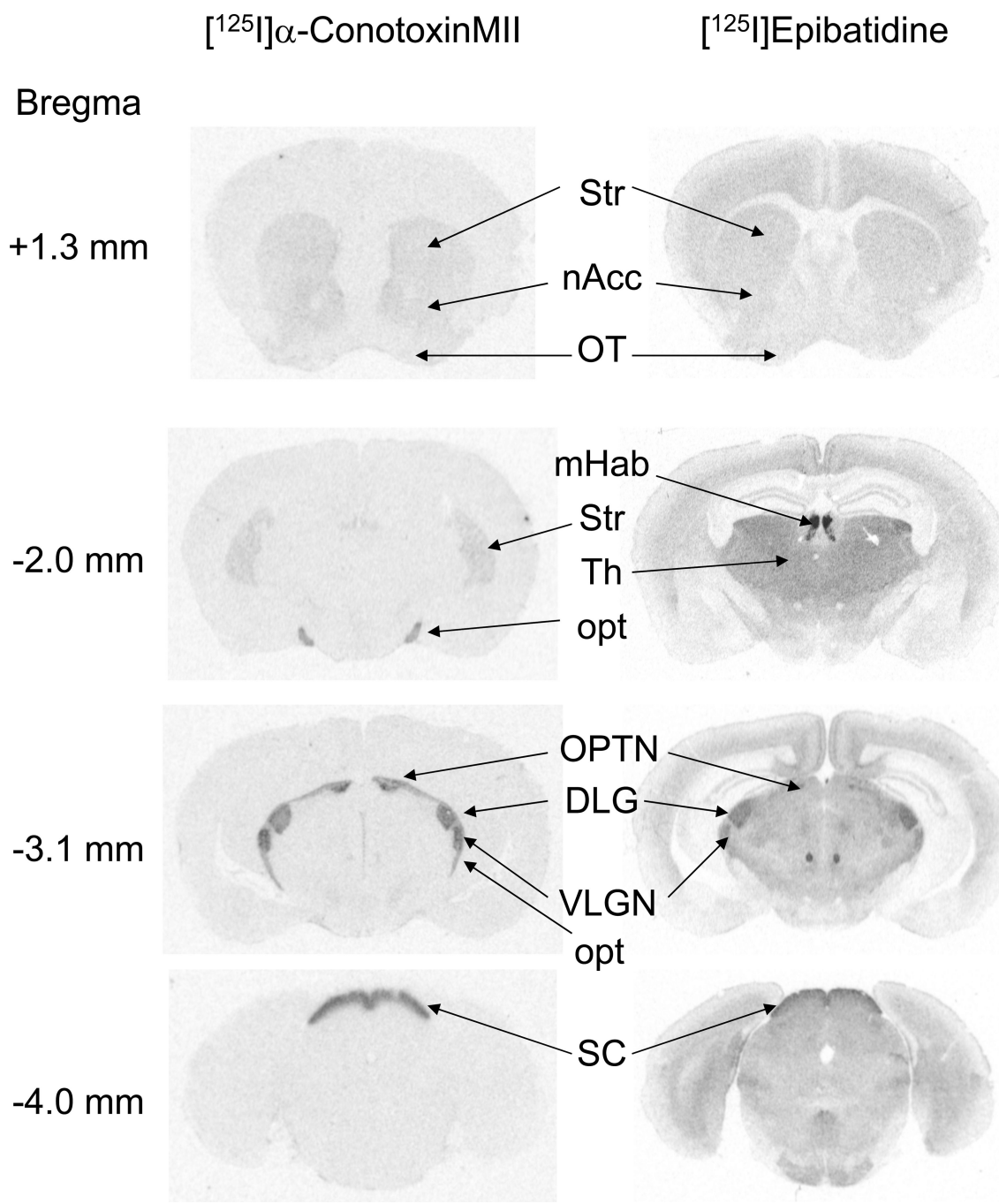

Figure 1. Autoradiograms of [^{125}I]α-conotoxinMII ([^{125}I]α-CtxMII) and [^{125}I]epibatidine binding

Representative examples are shown of radioligand binding patterns, recorded on X-ray film, using autoradiography approaches as described in the Methods section. Left column: [^{125}I]α-CtxMII (500 pM) labeling. Right column: [^{125}I]epibatidine (200 pM). Regions of interest are labeled as follows: DLG, dorsolateral geniculate nucleus; mHab, medial habunula; nAcc, nucleus accumbens; opt, optic tract; OPTN, olivary pretectal nucleus; OT, olfactory tubercle; SC, superior colliculus (superficial layers); Str, striatum; Th, thalamus; VLGN, ventrolateral geniculate nucleus.

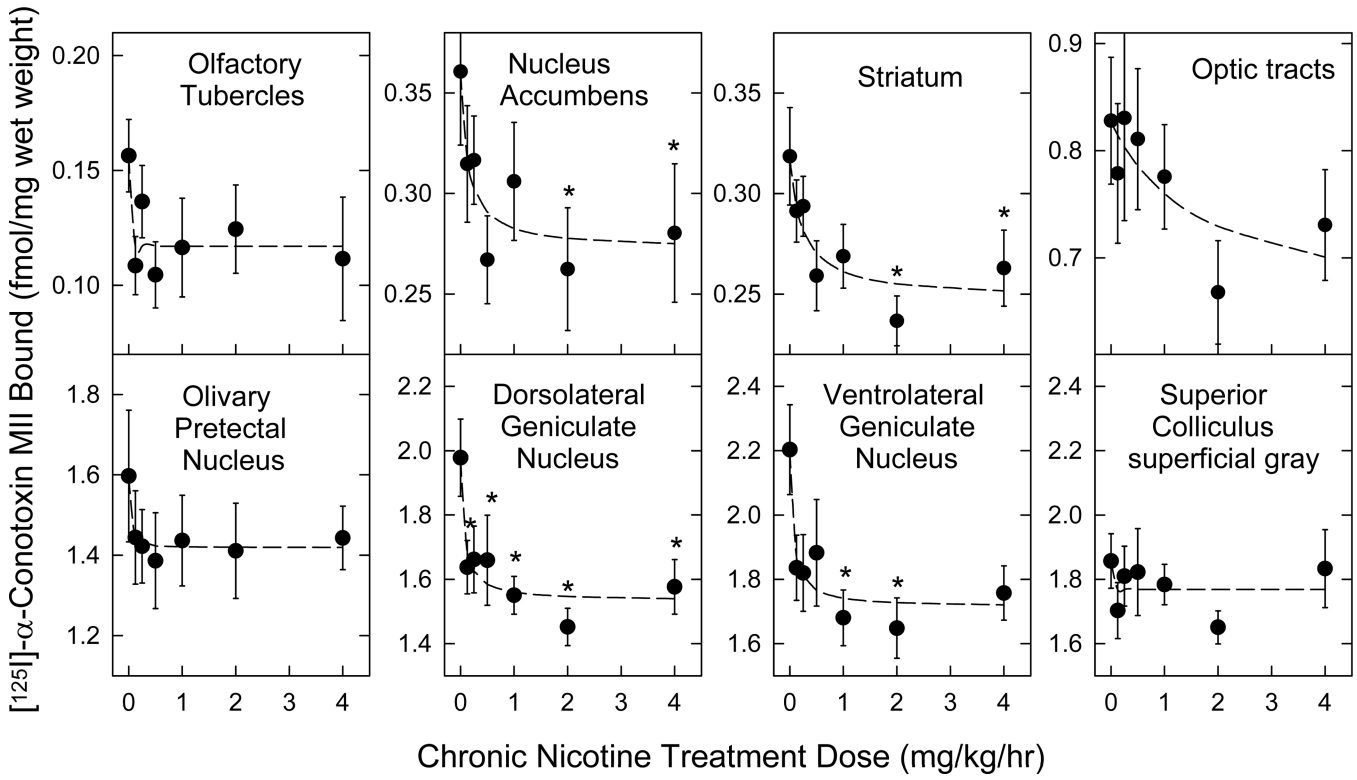

Figure 2. Concentration dependence of decreased [^{125}I]α-CtxMII binding site (α6β2* nAChR) expression following chronic nicotine administration

Mice were treated for 10 days with continuous infusion of sterile saline (control) or a range of nicotine doses (0.125 – 4 mg/kg/h). Expression of α6β2* nAChR was assessed using [^{125}I]α-CtxMII autoradiography in sections (14 μm) collected from each brain. Specific labeling was determined as the difference in labeling by quantitation of total binding (500 pM [^{125}I]α-CtxMII alone) and non-specific labeling (500 pM [^{125}I]α-CtxMII in the presence of 100 μM nicotine) between adjacent sections or equivalently by binding to sections of β2 null mutant mice, by reference to known radioactive standards. Please see Methods section for experimental details. n = 9 for each point; points represent mean ± S.E.M.; * denotes a significant difference ($p < 0.05$) from no-nicotine control binding detected by one-way ANOVA within each region, followed by the Duncan *post-hoc* test. All other statistical analyses and calculated parameters are given in Table 1.

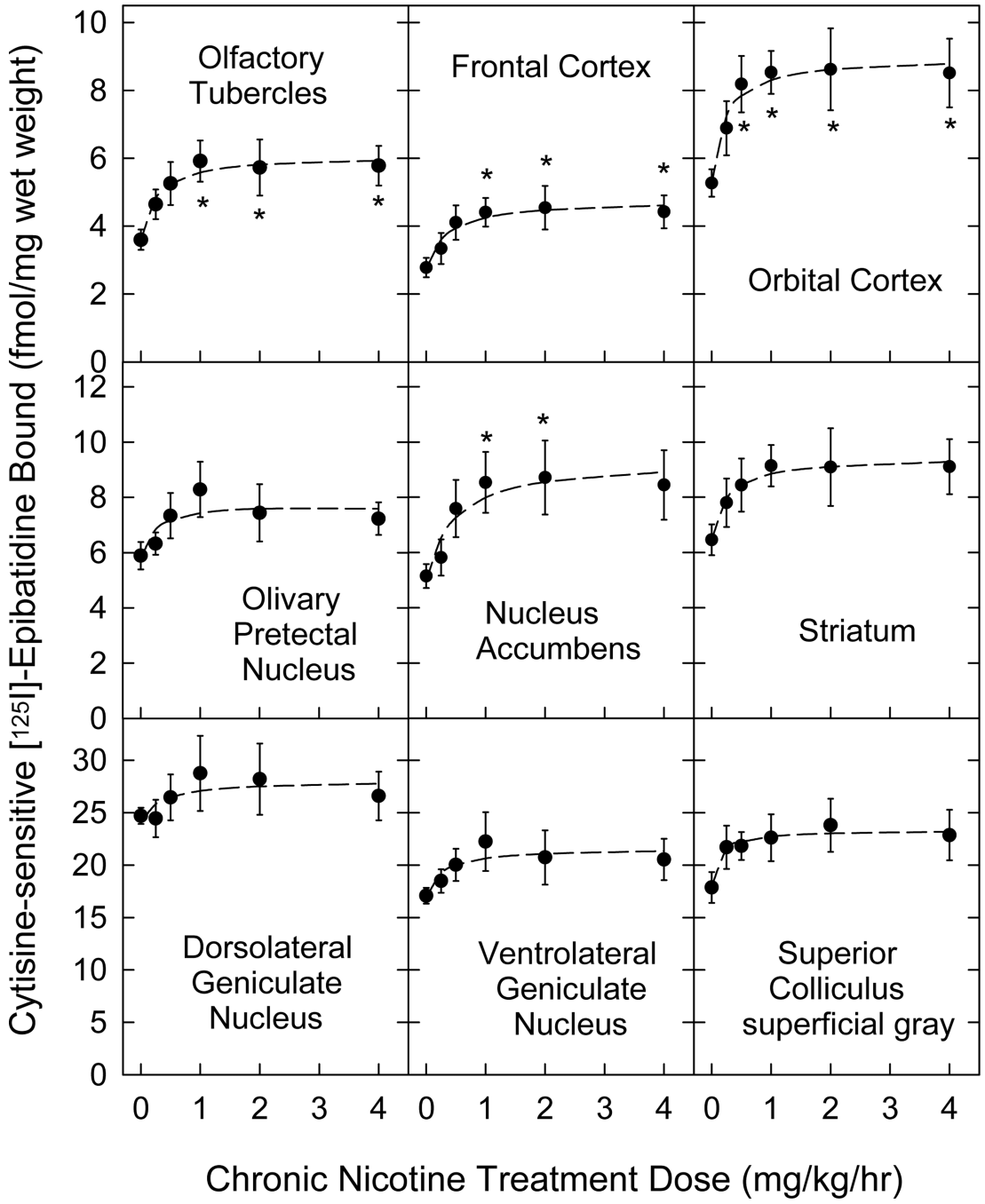

Figure 3. Concentration dependence of increased cytisine-sensitive [^{125}I]epibatidine binding site (α4β2* nAChR) expression following chronic nicotine administration

As in Figure 2, mice were treated for 10 days with continuous infusion of sterile saline (control) or a range of nicotine doses (0.125 – 4 mg/kg/h). Expression of α4β2* nAChR was assessed using [^{125}I]epibatidine autoradiography in sections (14 μm) collected from each brain. Specific labeling of α4β2* nAChR was determined as the difference in labeling by quantitation of total binding (200 pM [^{125}I]epibatidine alone) and cytisine-sensitive labeling (200 pM [^{125}I]epibatidine in the presence of 50 nM cytisine) between adjacent sections, by reference to known radioactive standards. Nonspecific binding measured by including 10

μM nicotine in the incubation did not differ from film background. Please see Methods section for experimental details. n = 5–6 for each point; points represent mean ± S.E.M; * denotes a significant difference ($p < 0.05$) from no-nicotine control binding detected by one-way ANOVA within each region, followed by the Duncan *post-hoc* test. All other statistical analyses and calculated parameters are given in Table 1.

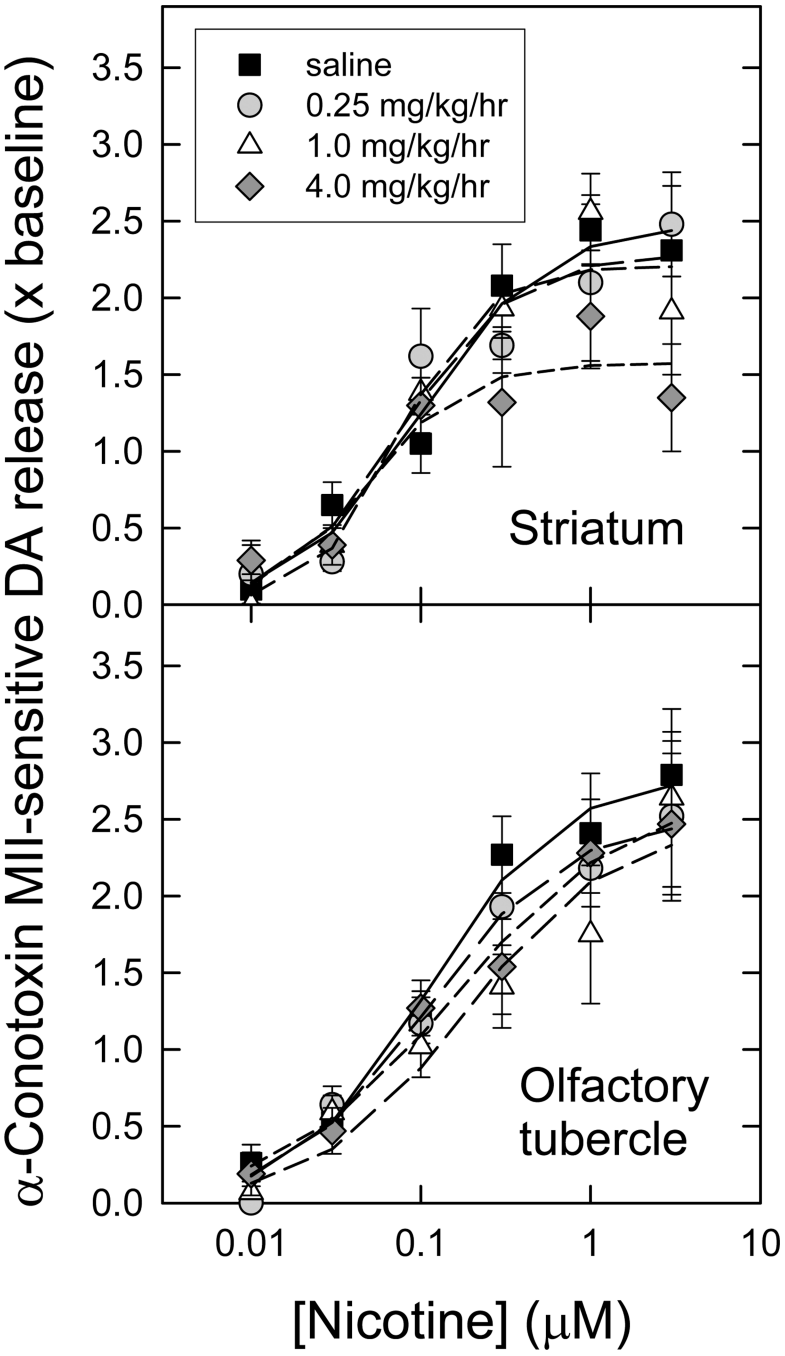

Figure 4. Concentration-response curves for nicotine-evoked [^{3}H]dopamine release mediated by α6β2* nAChR following chronic nicotine administration

Crude synaptosomes were produced from striatum and olfactory tubercles of animals treated for 10 d with saline (control) or three different nicotine doses as indicated. Synaptosomes were loaded with [^{3}H]-DA, then superfused for 5 min in the presence or absence of 50 nM α-CtxMII just prior to stimulation with a range of nicotine concentrations (10 nM – 3 μM). α-CtxMII-sensitive release (mediated by α6β2* nAChR) of [^{3}H]-DA was calculated by subtracting the resistant fraction from the total (n = 6–11 for each point; points represent mean values ± S.E.M), and is expressed as a multiple of baseline release just before

stimulation. The curves for stimulation by nicotine represent the best fits of the data as one saturable component, for each chronic treatment regime, in each region, as described in the Methods. Calculated parameters and statistical analyses are given in Table 2.

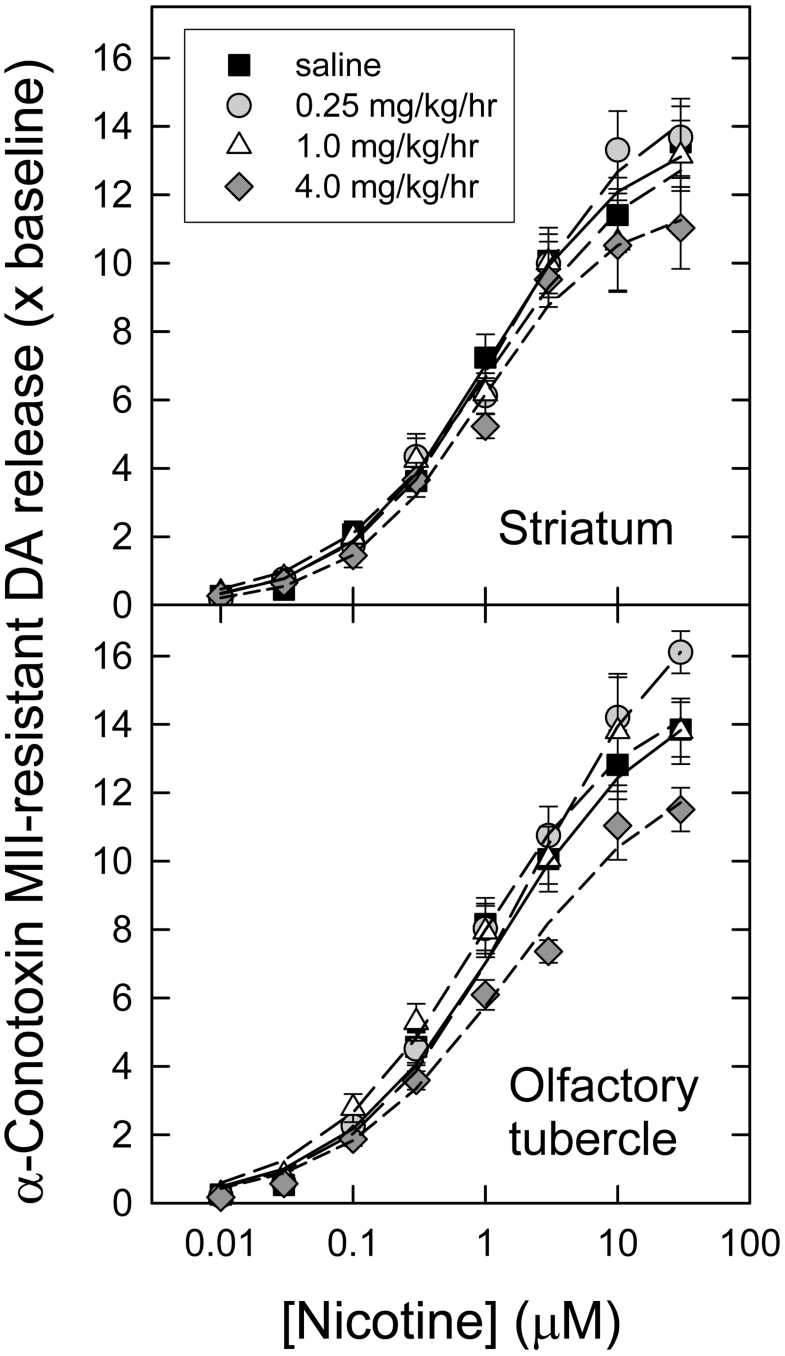

Figure 5. Concentration-response curves for nicotine-stimulated [^{3}H]dopamine release mediated by α4β2* nAChR following chronic nicotine administration

Crude synaptosomes were produced from striatum and olfactory tubercles of animals treated for 10 d with saline (control) or with the indicated different nicotine doses. Synaptosomes were loaded with [^{3}H]-DA, then superfused for 5 min in the presence of 50 nM α-CtxMII just prior to stimulation with a range of nicotine concentrations (10 nM – 3 μM). The residual α-CtxMII-resistant release of [^{3}H]-DA is mediated by α4β2* nAChR (n = 6–11 for each point; points represent mean values ± S.E.M), and is expressed as a multiple of baseline release just before stimulation. The curves for stimulation by nicotine represent the

best fits of the data as one saturable component, for each chronic treatment regime, in each region, as described in the Methods. Calculated parameters and statistical analyses are given in Table 2.

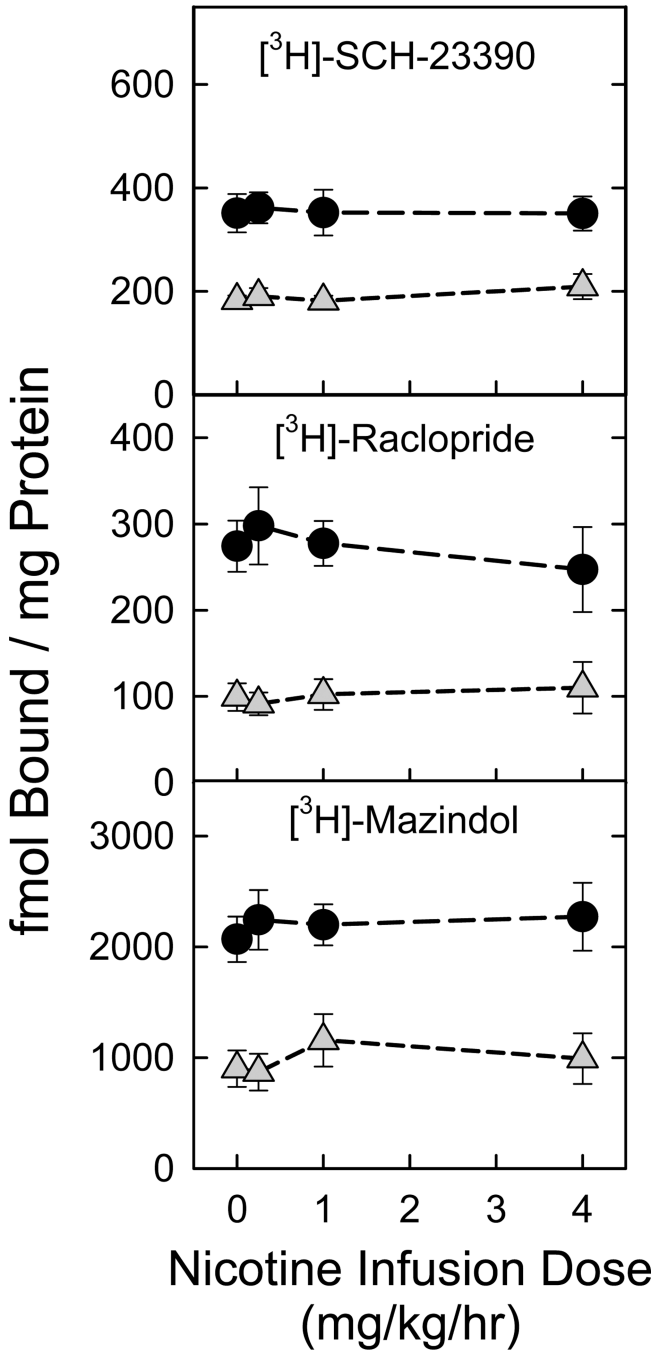

Figure 6. Chronic nicotine administration does not affect expression of dopamine system markers

Expression of dopaminergic markers was assessed in striatum and olfactory tubercle membrane preparations of animals treated for 10 d with saline (control) or with the three indicated nicotine doses. Values obtained in striatal membranes are represented as black circles, while those measured in olfactory tubercles are shown as gray triangles (n = 6–7 per point; points represent mean ± S.E.M.). Expression of D1/D5 receptors was measured using [^{3}H]-SCH23390 (1.7 nM; top panel), while that of D2/D4 receptors was measured using [^{3}H]-raclopride (17 nM; middle panel). Dopamine transporter (DAT) expression was

assessed by binding of [^{3}H]-mazindol (200 nM; lower panel). One-way ANOVA was performed for each marker in each region to determine if chronic nicotine treatment significantly affected expression levels. No effect of nicotine dose was seen in any combination of region × marker.

Table 1

Curve-fit parameters for chronic nicotine-induced changes (up- or down-regulation) of nAChR expression

Parameters are derived from curve fits performed in Figures 2 (for α6β2* nAChR; left column) and 3 (for α4β2* nAChR; right column).

Region	[^{125}I]α-CtxMII binding sites (α6β2* nAChR)		Cytisine-sensitive [^{125}I]-epibatidine binding sites (α4β2* nAChR)	
	ED_{50} (nM) / mg/kg/h	Max % change	ED_{50} (nM) / mg/kg/h	Max % change
OT	0.128 ± 0.057	−28.8 ± 13.4*	0.258 ± 0.130	71.1 ± 23.5
nAcc	0.136 ± 0.110	−23.9 ± 9.6*	.446 ± 0.212	89.5 ± 33.3
Str	0.241 ± 0.129	−22.0 6.7*	0.255 ± 0.170	47.2 ± 19.9
opt	ns	ns	ns	ns
OPTN	ns	ns	ns	ns
DLG	0.066 ± 0.045	−22.4 ± 6.7*	ns	ns
VLG	0.061 ± 0.047	−23.2 ± 6.2*	ns	ns
SCsg	ns	ns	ns	ns
fCX	nd	nd	0.339 ± 0.189	73.6 ± 25.7
inCX	nd	nd	0.208 ± 0.193	93.2 ± 29.9
orbCX	nd	nd	0.218 ± 0.116	71.8 ± 22.9
outCX	nd	nd	0.287 ± 0.160	61.4 ± 23.1
SCdl	nd	nd	ns	ns
Th	nd	nd	ns	ns
Overall for regions with changes	0.108 ± 0.040	−24.1 ± 1.2	0.293 ± 0.027	+72.5 ± 5.9

nd = not determined for reasons of undetectable binding; ns = un-measurable change by treatment. Two-way ANOVA was performed to determine the effects of Region and Dose on α6β2* nAChR downregulation following chronic nicotine treatment levels. Both factors significantly affected expression ($F[7,56] = 591$, $p < 0.001$ and $F[6,56] = 6.33$, $p < 0.001$, respectively), confirming that expression of α6β2* nAChR varies across brain regions, and is significantly affected by chronic nicotine treatment. No Region × Dose interaction was seen, however ($F[7,42] = 0.86$, $p < 0.727$), demonstrating that the dose dependence of α6β2* nAChR downregulation is generally similar for each region. Results were further analyzed to calculate the nicotine treatment dose dependence on binding site densities for each brain region as described in the Methods. Significant and similar extents of downregulation were observed for five of the eight brain regions. The means ± SEM for the maximum percentage decreases shown are significantly less than zero as determined by t-test for that parameter calculated from the non-linear least-squares curve fits. Accordingly, a mean ED_{50} downregulation nicotine dose was calculated for those five brain regions. Expression of α4β2* nAChR was generally upregulated, in contrast to the effects recorded for α6β2* nAChR. Two-way ANOVA showed that both Region ($F[12,91] = 104$, $p < 0.001$) and Dose ($F[6,91] = 3.08$, $p = 0.006$) significantly affected expression of this receptor population. Again, no Region×Dose interaction was observed ($F[12,72] = 0.27$, $p = 1$). Results were further analyzed to calculate the nicotine treatment dose dependence for the increase in binding site densities as described in the Methods. Significant upregulation was detected in seven of the fourteen regions analyzed. The means ± SEM for the maximum percentage decreases shown are significantly greater than zero as determined by t-test for that parameter calculated from the non-linear least-squares curve fits. Mean ED_{50} values for nicotine-induced upregulation were also calculated for these regions. By t-test, the ED_{50} values for α6β2* nAChR downregulation are significantly different from the ED_{50} values for the α4β2* nAChR upregulation ($t=5.23$, degrees-of-freedom = 12; $p < 0.001$). Regions of interest are labeled as follows: Regions of interest are labeled as follows: DLG, dorsolateral geniculate nucleus; fCX, frontal cortex; in CX, inner layers of cortex; nAcc, nucleus accumbens; opt, optic tract; OPTN, olivary pretectal nucleus; orbCx, orbital cortex; outCx, outer layers of cortex; OT, olfactory tubercle; SCdl, superior colliculus (deep layers); SCsg, superior colliculus (superficial grey); Str, striatum; Th, thalamus; VLG, ventrolateral geniculate nucleus.

Table 2

Curve-fit parameters for DA release (all Hill fit numbers)

Parameters are derived from curve fits performed in Figures 4 (for α6β2* nAChR) and 5 (for α4β2* nAChR).

α6β2*-nAChR Treatment	EC_{50}	Rmax	n_H	EC_{50}	Rmax	n_H
	ST	ST	ST	OT	OT	OT
Saline	0.099 ± 0.026	2.48 ± 0.19	1.21 ± .032	0.110 ± 0.024	2.79 ± 0.18	1.12 ± 0.22
0.25 mg/kg/h nicotine	0.077 ± 0.030	2.28 ± 0.25	1.32 ± 0.56	0.107 ± 0.027	2.51 ± 0.18	1.07 ± 0.23
1.0 mg/kg/h nicotine	0.075 ± 0.023	2.21 ± 0.20	1.75 ± 0.77	0.181 ± 0.121	2.47 ± 0.50	1.00 ± 0.49
4.0 mg/kg/h nicotine	0.048 ± 0.022	1.57 ± 0.20*	1.54 ± 0.87	0.156 ± 0.057	2.68 ± 0.27	0.84 ± 0.18
α4β2*-nAChR Treatment	EC_{50}	Rmax	n_H	EC_{50}	Rmax	n_H
	ST	ST	ST	OT	OT	OT
Saline	0.98 ± 0.18	13.9 ± 0.6	0.81 ± 0.08	1.26 ± 0.44	15.3 ± 1.2	0.71 ± 0.11
0.25 mg/kg/h nicotine	1.34 ± 0.35	15.4 ± 1.0	0.77 ± 0.10	2.10 ± 0.60	18.7 ± 1.4	0.69 ± 0.08
1.0 mg/kg/h nicotine	1.14 ± 0.40	13.9 ± 1.2	0.71 ± 0.11	0.87 ± 0.24	15.2 ± 1.0	0.72 ± 0.10
4.0 mg/kg/h nicotine	0.90 ± 0.22	11.8 ± 0.8*	0.89 ± 0.14	1.47 ± 0.56	13.2 ± 1.2*	0.68 ± 0.10

One-way ANOVA was performed comparing each parameter across treatment conditions, for each region. Where significant effects of treatment were detected, Duncan's post-hoc test was used to identify which treatment condition(s) produced significantly different parameter values compared to saline controls ($P<0.05$; indicated by *). Significant differences were only seen at the highest nicotine dose used (4.0 mg/kg/h), and were restricted to a subset of R_{max} values, as follows:

α6β2*-nAChR significant difference seen for striatal R_{max} ($F_{3,11}=10.41$, $P=0.004$).

α4β2*-nAChR significant difference seen for striatal R_{max} ($F_{3,11}=7.54$, $P=0.010$), and for olfactory tubercle R_{max} ($F_{3,11}=9.39$, $P=0.005$).

Table 3

[^{3}H]-DA Uptake after chronic treatment

Rate of uptake was determined from 5 min incubations. Total equilibrium uptake was determined at 30 min. Both assays were conducted at room temp, with synaptosomal preparations from mice chronically treated with saline, 0.5 or 4 mg/kg/h nicotine (n=6,7,6 mice, respectively).

Chronic Treatment	Rate of uptake using 0.05 µM DA fmol/mg/min	Rate of uptake using 1.0 µM DA fmol/mg/min	Total uptake using 0.05 µM DA fmol/µg	Total uptake using 1.0 µM DA fmol/µg	Ratio of high DA/low DA for rate	Ratio of high DA/low DA for total
STRIATUM						
Saline (control)	14.6 ± 0.8	43.4 ± 7.2	181 ± 16	378 ± 32	2.98 ± 0.46	2.15 ±0.18
Nic 0.5 mg/kg/h	15.2 ± 1.5	33.9 ± 2.4	171 ± 25	319 ± 24	2.47 ± 0.46	2.15 ± 0.36
Nic 4.0 mg/kg/h	16.5 ± 3.4	39.4 ± 3.6	232 ± 50	459 ± 58	3.00 ± 0.85	2.50 ± 0.56
OLFACTORY TUBERCLES						
Saline (control)	9.6 ± 2.3	26.7 ± 3.2	131 ± 24	208 ± 33	3.58 ± 0.97	1.70 ± 0.31
Nic 0.5 mg/kg/h	10.2 ± 1.3	22.3 ± 3.1	123 ± 20	211 ± 25	2.21 ±0.23	1.85 ± 0.24
Nic 4.0 mg/kg/h	12.6 ± 2.0	32.9 ±2.7	166 ± 34	349 ± 31*	2.85 ± 0.34	2.57 ± 0.55

One-way ANOVA and Duncan's post-hoc test 32 was used to identify any significant differences (*P<0.05) treatment-induced differences from saline-treated control for each parameter within each region. Only one significant change was identified: an increase in total olfactory tubercle synaptosomal uptake following 4.0 mg/kg/h nicotine treatment ($F_{2,17}$=7.671, P=0.005). We have previously determined the K_m for C57 mouse DA uptake to be 0.080 ± 0.003 µM DA; the ratio of ~K_m conc/ saturating conc gives an estimate of whether the K_m has changed. Ratios are not different by region or treatment in two-way ANOVA. A constant ratio of approximately 2 indicates that our estimate of K_m is accurate and does not change under any of the experimental conditions.